Journal of Ceramic Processing Research. Vol. 19, No. 4, pp. 355~359 (2018)

J O U R N A L O F
Ceramic Processing Research

Effects of gelation temperature, water, polyethylene glycol on morphology of ZrB_2 particles synthesized by sol-gel method

Yun Zhang* and Hong·Sun
Department of applied chemistry, Yuncheng University, Shanxi, People's Republic of China, 044000

Zirconium diboride (ZrB_2) ceramic material has many excellent properties and gains great importance in variety of applications. In the present work, the influence of the gelation temperature, H_2O, and polyethylene glycol on the morphology of ZrB_2 particles was investigated. Increasing the gelation temperature, the particle shapes changed from sphere-like particles at 65 °C to a particle chain at 75 °C, and then form rod-like particles at 85 °C. Moreover, different concentration of polyethylene glycol with 1 and 3 M was added, the morphology of ZrB_2 particles was prism and sphere-like, respectively. When the polyethylene glycol was added with 3 M, the reunion between particles was obviously lowered. Furthermore, different amount of water with 4, 6, and 10 ml was added, the shape of ZrB_2 particles was sphere-like and the average grain diameter was changed from 65, 25, to 20 nm.

Key words: Gelation temperature, Polyethylene glycol, H_2O, Morphology, Zirconium diboride.

Introduction

Zirconium diboride (ZrB_2) is one of the materials known as ultra-high-temperature ceramics. It has a series of excellent properties, such as a high melting temperature (3250 °C), high hardness (23 GPa), flexural strength (>500 MPa) [1], high thermal (60-140 W/(mK)), and electrical conductivity (~10^7 S/m)[2] because of the coexistence of covalent and metallic bond. The unique combination of properties makes ZrB_2 a promising candidate for thermal protection materials, cutting tools, high temperature electrodes, and molten metal crucibles [3-7].

Up to now, one-dimensional (1D) materials have attracted considerable attention because of their outstanding optical, electrical, and mechanical properties. In particular, studies about the synthesis and application of 1D SiC and Si_3N_4 have been widely reported. As reported by Li [8], SiC whisker reinforced reaction bonded SiC composites with increased toughness have been developed. Likewise, Hirao et al [9]. fabricated self-reinforced Si_3N_4 with a preferred oriedtation of elongated grains showing increased fracture toughness (1101 MPa·$m^{1/2}$) and bending strength (1100 MPa) by seeding with rod-like β-Si_3N_4 particles. Similar to SiC and Si_3N_4, 1D ZrB_2 was recently reported to be an effective reinforcement to improve the fracture toughness of the ZrB_2-based composites, such as ZrB_2-ZrCx [10], ZrB_2-$MoSi_2$ [11], and ZrB_2-SiC-WC [12]. Therefore, 1D ZrB_2 may have great potentials for application and the synthesis of 1D ZrB_2 is attractive.

At present, several different researchers have showed interest in synthesizing ZrB_2 powders using different methods to change the sintering performance and oxidation resistance, but few literatures reported ZrB_2 shapes [13-15]. For instance, Li [16] prepared ZrB_2 with nanofibers by carbothermal reduction via electrospinning using polyzirconoxane, H_3BO_3, and polyacrylonitrile. Li et al [17]. synthesized ZrB_2 with plate shapes by solid-state method using ZrO_2, H_3BO_3, and carbon. In our previous work [18], ZrB_2 particles with different shapes (equiaxed, chain, and rod) have been synthesized by sol-gel method using $Zr(OPr)_4$, H_3BO_3, $C_{12}H_{22}O_{11}$, and AcOH. In this study, the morphology of ZrB_2 with sphere-like, chain, rod-like, and prism has been synthesized by sol-gel method through changing the gelation temperature, adding polyethylene glycol (*PEG*), and adding different amount of H_2O.

Experimental and Method

Starting materials

$Zr(OPr)_4$ was supplied by the Shanghai Jingchun Reagents Co. Ltd., Shanghai, China. H_3BO_3, $C_{12}H_{22}O_{11}$, acetic acid (AcOH), methanol (CH_3OH), polyethylene glycol 400 (*PEG*), and acetylacetone (*acac*) were supplied by the Lanyi Reagents Co. Ltd., Beijing, China. The grade of all the above reagents was analytical.

Synthesis

According to the literature [19], the synthesis of ZrB_2

*Corresponding author:
Tel : +861082316500
E-mail: zhangyun0320@126.com

powder is shown as follows: 6.3 ml of $Zr(OPr)_4$ was dissolved in a stirred mixture solution of 25 ml CH_3OH and 1.2 ml *acac* at room temperature. Then, 4.0 ml (6 ml and 10 ml were also in the final section of this paper) of distilled water was dropwise added and this resulting solution was continuously stirred for 30 min. We refer to this solution as Solution 1. On the other hand, 2.5 g of H_3BO_3 and 2.9 g of $C_{12}H_{22}O_{11}$ were dissolved in 45 ml of AcOH using another beaker. Then, it was heated with vigorous stirring to 80 ºC and maintained for 0.5 h. This was Solution 2. Afterwards, the Solution 1 was carefully decanted to the Solution 2 after the Solution 2 previously cooled to room temperature. This was Solution 3. The resulting Solution 3 was heated with vigorous stirring to 65 ºC (This fixed temperature is so-called gelation temperature to form sol/gel. 75 ºC and 85 ºC were also set in the final section of this paper.) and maintained for 4 h to form a wet gel. Finally, it was dried under vacuum at 120 ºC for 3 h followed by a grind process using an agate mortar and a pestle. In this way, a precursor was prepared. This synthesis powder was called Sample 1.

For purposes of comparison, when adding 4 ml of water was fixed, the gelation temperature was changed from 65, 75, to 85 ºC, the synthesis powders were called Sample 2 (75 ºC) and Sample 3 (85 ºC), respectively. When the gelation temperature was fixed at 65 ºC, the amount of H_2O was changed from 4, 6, to 10 ml, the synthesis powders were called Sample 4 (6 ml) and Sample 5 (10 ml), respectively. Based on Sample 1, the different concentration of *PEG* with 1 and 3 M was added to Solution 3, the synthesis powders were called Sample 6 (1 M) and Sample 7 (3 M), respectively.

After that, the above precursors were firstly heated to 800 ºC at a heating rate of 5 ºC / min, then to 1200 ºC at 3 ºC / min and maintained at this temperature for 2 h in argon using an alumina tube furnace. Afterwards, the precursor was continued to heat from 1200 ºC to 1550 ºC at a heating rate of 2 ºC / min and held at this temperature for 2 h. Then, the sample was cooled to room temperature at a cooling rate of 5 ºC / min. In the end, gray powders were obtained.

Characterization

The crystallographic constitution was identified by means of an X-ray diffractometer (XRD) using graphite monochromatized CuK_a radiation (Rigaku, D/MAX 2200 PC). Crystallite size was estimated using the Debye-Scherer equation,

$$D_{hkl} = 0.9\lambda / \beta_{hkl} \cos\theta \quad (1)$$

Where D_{hkl} is the crystallite size, λ is the wavelength of Cu Kα radiation, β_{hkl} is the full-width at half maximum, and θ is the Bragg diffraction angle. The morphology of the final products was characterized by SEM using a JEOL JSM-6700F JAPAN microscope and TEM using a JEM-2100F microscope.

Results and Discussion

Structure and composition characterization

It is well known that the gelation temperature and the amount of H_2O were important factors for both nucleation and crystal feature. Moreover, surfactant can change the reunion between the particles. Here, different gelation temperatures, different amount of H_2O, and different concentration of *PEG* were fixed to synthesize ZrB_2 powders.

According to the literature [19], a single phase of ZrB_2 without residual ZrO_2 was evolved at 1550 ºC for 2 h. Fig. 1 shows XRD patterns of the Sample 1, 2, 3, 4, 5, 6, and 7 calcined at 1550 ºC for 2 h, respectively. It might be seen that all of the diffraction peaks were well assigned to a single phase of ZrB_2.

Morphology characterization

Influence of gelation temperature on morphology of ZrB_2

According to the literature [18], it was observed that the morphology of ZrB_2 has changed with different gelation temperature from sphere-like at 65 ºC to particle chain at 75 ºC, and rod-like at 85 ºC. Here, the influence of the gelation temperature on the morphology of the samples was also investigated, and the SEM images of the as-calcined samples are shown in Fig. 2. It is observed that the morphology of the samples was affected by the gelation temperature. For the ZrB_2 sample gelated at 65 ºC, the SEM revealed a sphere-like morphology of ZrB_2 nanoparticles (*see* Fig. 2(a)). At 75 ºC, the morphology showed a particle chain (*see* Figs. 2(b) and 3(a)). With the increasing of the temperature to 85 ºC, the morphology of the ZrB_2 particles evolved to a rod-like shape (*see* Figs. 2(c) and

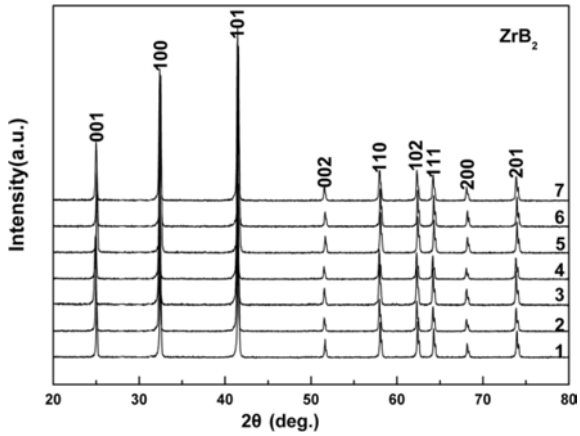

Fig. 1. XRD patterns of the precursor powder reduced carbothermally at 1550 °C for 2 h with gelation temperatures of (1) 65 °C; (2) 75 °C; (3) 85 °C; the amount of water(4) 6 ml; (5) 10 ml; the concentration of *PEG* (6) 1 M; (7) 3 M.

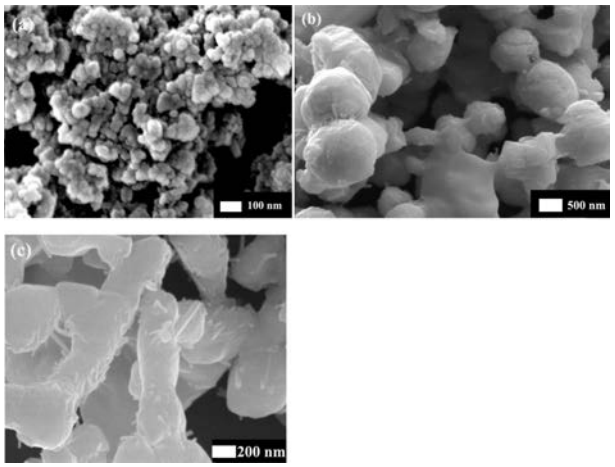

Fig. 2. SEM images of ZrB_2 powder reduced carbothermally at 1550 °C for 2 h with gelation temperatures of (a) 65 °C; (b) 75 °C; (c) 85 °C.

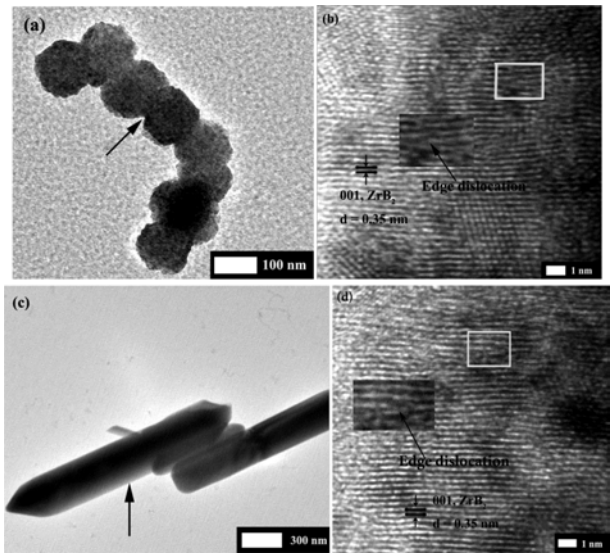

Fig. 3. TEM images of ZrB_2 powder reduced carbothermally at 1550 °C for 2 h with gelation temperatures of (a) 75 °C; (c) 85 °C; (b) HRTEM image of ZrB_2 particle chain marked in (a); (d) HRTEM images of rod-like ZrB_2 marked in (c).

3(c)). Additionally, the size of ZrB_2 particle also increased notably with the increasing of the gelation temperature.

To explain the morphology influenced by the gelation temperature requires a multidisciplinary knowledge. According to the literature [18], a further investigation, a high-resolution TEM (HRTEM), was conducted to clarify the microstructure and crystal feature of the ZrB_2 particles. At a lower temperature, the rate of nucleation was faster than that of growth, whereas the monomer concentration was sharply decreased [20]. Such slow growth conditions favored the formation of a sphere-like shape (*see* Fig. 2(a)). With increasing the gelation temperature, Figs. 2(b) and 3(a) show that a particle chain of ZrB_2 was evolved at 75 °C. The HRTEM image of ZrB_2 particle chain revealed that

Table 1. The morphology and phase composition of powder with different amount of H_2O and the corresponding gelation time.

Amount of H_2O (ml)	4	6	10
Gelation temperature (°C)	65	65	65
Gelation time (h)	4	6	8
Calcinati on temperature (°C)	1550	1550	1550
Morphology	sphere-like	sphere-like	sphere-like
Average grain diameter (nm)	62	25	20

each unique particle chain was composed of several sphere-like particles. These sphere-like particles aligned one by one to form a polycrystalline particle chain of ZrB_2 and shared a quasi-parallel crystal orientation at the grain interfaces (*see* Figs. 3(a, b)). It is notable that the interface between the two grains in the rectangle region (magnified in Fig. 3(b)) involved edge dislocations (arrowhead). With the temperature further increased, adjacent particles fused together to form strong links resulting in the evolution of ZrB_2 rods (*see* Figs. 2(c) and 3(c, d)). In the same way, the adjacent grains shared a common crystallographic orientation, followed by joining of these grains at a planar interface with edge dislocations (arrowhead) (*see* Fig. 3(d)). It also may be found from the HRTEM image that these particle chain/rod shared {001} lattice fringes with interplanar spacings of 0.35 nm.

From a crystallography perspective, according to the "oriented attachment mechanism", which was first explored by Banfield [21], adjacent particles share a common crystallographic orientation, followed by joining of these particles at a planar interface. Bonding between adjacent nanoparticles reduces the overall energy by removing the surface energy associated with unsatisfied bonds. Clearly, this attachment mechanism is reflected by the results in Fig. 3. The ZrB_2 nanoparticles connected with each other via the "oriented attachment mechanism" and a reduction in surface free energy was achieved by the complete removal of pairs of surfaces. Imperfect oriented attachment of nanocrystals can generate dislocations. Any defects observed by HRTEM can be attributed to the growth process.

Influence of the amount of H_2O on morphology of ZrB_2

Theoretically, metal organic compounds forming process of sol and gel is essentially a hydrolysis process. The speed of formation sol-gel, the growth of crystal, and the morphology of ZrB_2 particles may be influenced by the different amount of H_2O. In the present work, when the gelation temperature was fixed at 65 °C, adding the different amount of H_2O from 4, 6, to 10 ml was investigated, respectively. From Fig. 1 (4) and Fig. 1(5), all of the diffraction peaks were well assigned to a single phase of ZrB_2. Moreover, when the gelation temperature and the calcination temperature

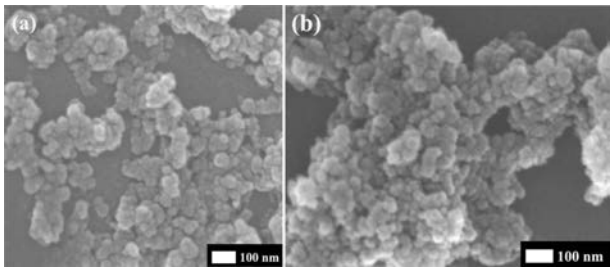

Fig. 4. SEM images of ZrB_2 powder reduced carbothermally at 1550 °C for 2 h with different amount of water (a) 6 ml; (b)10 ml.

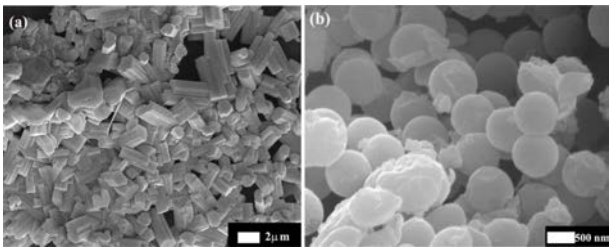

Fig. 5. SEM images of ZrB_2 powder reduced carbothermally at 1550 °C for 2 h with different concentration of *PEG* (a) 1 M; (b) 3 M.

were fixed, adding the amount of H_2O from 4, 6, to 10 ml, the gelation time was changed from 4, 6, to 8 h, and the average grain diameter was changed from 65, 25, to 20 nm, respectively (*see* Tab. 1).

Furthermore, the morphology of Sample 1, 4 and 5 were sphere-like (*see* Fig. 2(a) and Fig. 4). Here, adding the different amount of H_2O has not changed the morphology of ZrB_2, but the average grain diameter became smaller and the reunion of particles was serious. In order to explain the phenomenon of reunion, Ready [22] thought that the hydrogen bonds from H_2O molecules with the hydroxyl from the particles of the surface formed the bridge bonds. Those bridge bonds determined the size of reunion force between particles. When the particle was close to another particle, through the interaction of the hydrogen bonds and hydroxyl, and when the powder was dry, the H_2O molecules took off, and because of the close to each other to form chemical bonds between particles, eventually the hard reunion was produced [23].

Influence of the polyethylene glycol on morphology of ZrB_2

In the synthesis process, the morphology and size of particles were influenced by its environment. To stabilize the particles dispersed in the liquid system mainly reduced attractive force and increased the repelling force to control the particle / liquid bead forming gathered or flocculation. That process could be achieved by using nonionic surfactants or polymeric surfactants. Here, *PEG* was used to change the reunion between particles.

Fig. 1(6) and (7) show that all of the diffraction peaks were well assigned to a single phase of ZrB_2 and Fig. 5 shows that the morphology of ZrB_2 was prism and sphere-like. Obviously, the reunion was lowered between the particles by adding 3 M of *PEG* (*see* Fig. 5(b)), but the average grain diameter became bigger.

To explain the mechanism of forming different morphology of ZrB_2 was that *PEG* was a kind of nonionic surfactant and did not exist in the form of ions in the solution, therefore, its stability was very high. In the anhydrous state, polyoxyethylene chain of *PEG* was in zigzag state, when it was soluble in water, the weak hydrogen bonds were formed though the oxygen atoms of ether bond with the hydrogen of H_2O, and the molecular chains were twists and turns. The oxygen atoms of hydrophilic were located in the outer edge of the chain and ethenyl (*-CH_2CH_2-)* was located in the inner edge of the chain, thus, the chain around was just a hydrophilic entirety [24, 25]. In the crystal growth process, the hydrophilic group of *PEG* interacted with different crystal face of ZrO_2 particles lead to changing the growth speed of different crystal directions of ZrO_2 particles. Because of the different concentration of *PEG*, the number of *PEG* adsorbed around the ZrO_2 particles and the interfacial tension were different. Generally, the morphology of particles with the increasing of surfactant concentration more tended to form the rules of the morphology. Therefore, there were two shapes of ZrB_2 particles.

After adding *PEG*, ZrO_2 particles were parceled by *PEG* and formed the space barriers because of the adsorption. That is to say, that space barriers could prevent the collisions and union each other between particles, therefore, the reunion between particles could be lowered (*see* Fig. 5(b)).

Conclusions

In summary, sphere-like, particle chain, rod-like, and prism ZrB_2 particles could be obtained through different gelation temperatures (65, 75, and 85 °C), different concentration of *PEG* (1 and 3 M), and different amount of H_2O (4, 6, and 10 ml). In an effort to understand the mechanism of morphology evolution at different gelation temperatures, the "oriented attachment mechanism" might explain the crystalline processes of ZrB_2 particles based on the HRTEM observation. Moreover, the reunion between particles was obviously lowered by adding 3 M of *PEG*. Furthermore, the amount of H_2O with 4 and 6 ml was added, the average grain diameter was 25 and 20 nm, respectively.

Acknowledgments

This work was supported by Aerospace Materials and Technology Research Institute and National Science Foundation in China (No.51272009 and No.51072010), and College Program of YunCheng

University (No.097-081702).

References

1. J. W. Zimmermanm, G. E. Hilmas, W. G. Fahrenholtz, Thermaphysical properties of ZrB_2 and ZrB_2-SiC ceramics, J. Am. Ceram. Soc. 91 (2008) 1405-1411.
2. R. A. Cutler, in: Schneider SJ (Ed), Ceramics and glasses, engineered materials handbook, ASM International, Materials Park, OH, 4 (1992) 787-803.
3. W. G. Fahrenholtz, G. E. Hilmas, I. G. Talmy, J. A. Zaykoski, Refractory diborides of zirconium and hafnium, J. Am. Ceram. Soc. 90(2007) 1347-1364.
4. S. R. Levine, E. J. Opila, M. C. Halbig, J. D. Kiser, M. Singh, J. A. Salem,Evaluation of ultra-high temperature ceramics foraeropropulsion use, J. Eur. Ceram. Soc. 22 (2002) 2757-2767.
5. M. M. Opeka, I. G. Talmy, J. A. Zaykoski, Oxidation-based materials selection for 2000 °C hypersonic aerosurfaces: theoretical considerations and historical experience, J. Mater. Sci. 39 (2004) 5887-5904.
6. S. Norasetthekul, P. T. Eubank, W. L. Bradley, B. Bozkurt, B. Stucker, Use of zirconium diboride-copper as an electrode in plasma applications, J. Mate. Sci. 34 (1999) 1261-1270.
7. P. Anish, D. D. Jayaseelan, S. Venugopal, E. Zapata-Solvas, J. G. P. Binner, V. Bala, A. Heaton, P. Brown, W. E. Lee, UHTC composites for hypersonic applications, Am. Ceram. Soc. Bull. 91 (2012) 22-28.
8. S. Li, Y. Zhang, J. Zhou, Fabrication and characterization of SiC whisker reinforced reaction bonded SiC composite, Ceram. Int. 39 (2013) 449-455.
9. K. Hirao, M. Ohashi, M. E. Brito, S. Kanzaki, Processing strategy for producing highly anisotropic silicon nitride, J. Am. Ceram. Soc. 78 (1995) 1687-1690.
10. L. Xu, C. Huang, H. Liu, B. Zhou, H. Zhu, G. Zhao, J. Wang, In situ synthesis of ZrB_2-ZrC_x ceramic tool materials toughened by elongated ZrB_2 grains. Mater. Design 49 (2013) 226-233.
11. W. Wu, Z. Wang, G. Zhang, Y. Kan, P. Wang, ZrB_2-$MoSi_2$ composites toughened by elongated ZrB_2 grains via reactive hot pressing, Scripta Mater. 61 (2009) 316-319.
12. J. Zou, G. Zhang, Y. Kan, Formation of tough interlocking microstructure in ZrB_2-SiC-based ultrahigh-temperature ceramics by pressureless sintering, J. Mater. Res. 24 (2009) 2428-2434.
13. E. Jung, J. Kim, S. Jung, S. C. Choi, Synthesis of ZrB_2 powders by carbothermal and borothermal reduction, J. Alloy. Comp. 538 (2012) 164-168.
14. H. Qiu, W. Gou, J. Zou, G. Zhang, ZrB_2 powders prepared by boro/carbothermal reduction of ZrO_2: the effects of carbon source and reaction atmosphere, Powder Technol. 217 (2012) 462-466.
15. B. Y. Yang, J. P. Li, B. Zhao, Y. Z. Hu, T. Y. Wang, D. F. Sun, R. X. Li, S. Yin, Z. H. Feng, Q. Tang, S. Tsugio, Synthesis of hexagonal-prism-like ZrB_2 by a sol-gel route. Powder Technol. 256 (2014) 522-528.
16. F. Li, Z. Kang, X. Huang, G. J. Zhang, Synthesis of ZrB_2 nanofibers by carbothermal reduction via electrospinning, Chem. Eng. J. 234 (2013) 184-188.
17. R. X. Li, H. J. Lou, S. Yin, Y. Zhang, Y. S. Jiang, B. Zhao, J. P. Li, Z. H. Feng,Nanocarbon-dependent synthesis of ZrB_2 in a binary ZrO_2 and boron system, J. Alloy. Comp. 509 (2011) 8581-8583.
18. Y. Zhang, Y. S. Jiang, B. Zhao, H. P. Duan, J. P. Li, Z. H. Feng, Morphology evolution of ZrB_2 nanoparticles synthesized by sol-gel method, J. Solid State Chem. 184 (2011) 2047-2052.
19. R. X. Li, Y. Zhang, H. J. Lou, J. P. Li, Z. H. Feng, Synthesis of ZrB_2 nanoparticles by sol-gel method, J.Sol-Gel Sci. Techn. 58 (2011) 580-585.
20. L. Manna, E. C. Scher, A. P. Alivisatos, Synthesis of soluble and processable rod-, arrow-, teardrop-, and tetrapod-shaped CdSe nanocrystals, J. Am. Ceram. Soc. 122 (2000) 12700-12706.
21. R. L. Penn, J. F. Banfield, Imperfect oriented attachment: dislocation generation in defect-free nanocrystals, Science, 281 (1998) 969-971.
22. M. J. Readey, R. R. Lee, J. W. Halloran, Processing and sintering of ultrafine MgO-ZrO_2 and (MgO, Y_2O_3)-ZrO_2 powders, J Am. Chem. Soc. 73 (1990) 1499-1503.
23. M. M. Opeka, I. G. Talmy, J. A. Zaykoski, Mechnical, thermal and oxidation properties of refractory hafnium and zirconium compounds, J. Eur. Ceram. Soc. 19 (1999) 405-414.
24. H. S. Jahroml, H. Taghdisian, S. Afshar, S. Tasharrofi, Effects of pH and polyethylene glycol on surface morphology of TiO_2 thin film, Surf. Coat. Tech. 203 (2009) 1991-1996.
25. L. Zhang, Y. Zhu, Y. He, W. Li, H. Sun, Preparation and performances of mesoporous TiO_2 film photocatalyst supported on stainless steel, Appl. Catal. B: Environ. 40 (2003) 287-292.